2026 IEEE International Conference on Robotics and Automation (ICRA 2026)
June 1-5, 2026. Vienna, Austria

Moth: A Low-cost IR-based Approach Towards Autonomous Precision Drone Landing

Yanchen Liu*[1], Minghui Zhao*[1], Kaiyuan Hou[1], Junxi Xia[2], Charles Carver[1], Stephen Xia[2], Xia Zhou[1] and Xiaofan Jiang[1]

***Abstract*— As micro-drones become increasingly deployed in indoor environments for applications ranging from warehouse inspection to emergency response, the challenge of precise automated landing emerges as a crucial barrier to their practical operation and ubiquitous adoption. Existing landing approaches often require complex hardware and substantial computation or perform unreliably indoors, making them impractical for palm-sized microdrones. We propose Moth, a low-cost infrared light-based solution that targets precise and efficient landing of low-resource microdrones. Moth consists of an infrared light source at the landing station along with an energy-efficient photodiode (PD) sensing platform attached to the bottom of the drone. At a cost under 83 USD, Moth achieves comparable performance to vision-based methods but at a fraction of the energy consumption and computation. Moth requires only three PDs without any complex pattern recognition models to land the drone accurately, under 10 cm of error, from up to 11.1 m away.**

I. Introduction

The proliferation of drones in ubiquitous computing, from smart warehouses and hospital delivery systems [1], [2], [3] to factory asset tracking [4], [5], [6] and personal assistants [7], [8] , demands reliable autonomy in GPS-denied, dynamic environments. These applications often require compact, agile platforms. Palm-sized microdrones are uniquely suited for navigating challenging environments such as tight hospital corridors or cluttered factory floors. However, drones face significant operational constraints: consumer-grade models typically operate for only tens of minutes, while smaller indoor drones manage just a few minutes of flight time and can carry only tens of grams of payload [9], [10]. This creates a critical barrier to achieving precise landings for mission-critical operations, such as autonomously docking on charging stations or inspecting machinery, without relying on bulky, energy-intensive sensors that exceed the drone's power and weight budgets.

Existing landing approaches have proved impractical for such ubiquitous deployment of microdrones in everyday environments. Currently, most autonomous landing systems rely on GPS-based "return to home" functionality, which requires large landing areas to accommodate GPS inaccuracies and is ineffective indoors where GPS signals are blocked. While there are works that target drone landing using visual markers, wireless anchor points, or acoustic-based approaches, they often present trade-offs for palm-sized drones. For instance, while platforms like the Bitcraze Crazyflie can support UWB-based localization or carry lightweight AI decks for onboard image processing, these solutions can still impose constraints on the overall cost, payload, and power budgets of resource-constrained microdrones. Furthermore, vision-based processing often suffers in low-light environments, and UWB systems require specific hardware setups. Therefore, there remains a need for a landing system that prioritizes simplicity of setup, ease of deployment, ultra-low cost, and robust performance in visually degraded (e.g., low-light) environments.

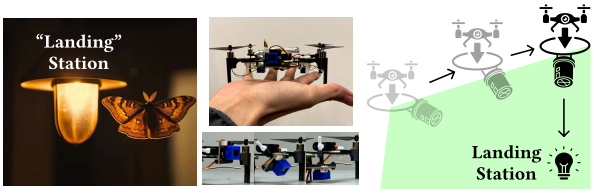

Fig. 1: Moth seeks light, lands drones precisely.

Leveraging infrared (IR) light to guide and land drones is advantageous over camera-based methods because IR lies outside the visible spectrum and is not affected by ambient light (e.g., at night). Existing IR-based guidance and landing systems generally use IR beacons along with an IR camera to perform pattern recognition. Like RGB camera-based systems, this requires comparatively expensive cameras.

We propose Moth, a low-cost, energy-efficient, IR-based platform for autonomous and precise drone landing, inspired by insects that seek light as shown in Figure 1. Moth targets microdrones that are often smaller than palm-size with low battery life to support active or high resolution sensing. Moth consists of two simple hardware components: 1) a landing station with an off-the-shelf IR light bulb, 2) a small PD array on the drone to guide it to land, even in partially non line of sight scenarios. Unlike camera-based methods that require hundreds of thousands of pixels to perform pattern recognition, Moth leverages weighted light intensity from multiple PDs at close range, and sweeping a single PD to detect light direction at long range. As such, Moth simply requires light intensity sensing without complex pattern recognition while acoustic and RF methods typically need to handle multipath issues. Our main contributions are as follows:

- **Low-cost and practical hardware-software IR landing**

[1]Yanchen Liu, Minghui Zhao, Kaiyuan Hou, Charles Carver, Xia Zhou and Xiaofan Jiang are with the Department of Electrical Engineering, Columbia University, USA {yl4189, mz2866, kh3119}@columbia.edu, {cjc, xia}@cs.columbia.edu, jiang@ee.columbia.edu
[2] Junxi Xia and Stephen Xia are with the Department of Electrical and Computer Engineering, Northwestern University, USA junxixia2024@u.northwestern.edu, stephen.xia@northwestern.edu
*Both authors contributed equally to this work

solution: We present Moth, a bio-inspired, end-to-end platform for precise autonomous landing targeting low-resource palm-sized microdrones. At a cost under 83 USD and weighing less than 18 g, it provides a highly accessible and easy-to-deploy alternative to more complex UWB or vision-based setups, particularly excelling in low-light environments.

- **Efficient guidance and landing exploiting the drone's mobility.** We introduce a novel bio-inspired method to guide the drone to the landing station by exploiting the drone's mobility and using onboard photodiodes (PDs). Unlike vision-based approaches that require complex pattern recognition, Moth steers the drone toward the highest light intensity using only a few PDs, enabling efficient and accurate landing with minimal computation.
- **Demonstration in real and partially non-line-of-sight settings.** We deploy Moth in a variety of realistic indoor environments, and demonstrate *comparable landing performance* to existing vision-based approaches at a *fraction of the energy cost* (μW level vs mW level for vision-based methods), from up to 11.1 m from the landing station. Moreover, we demonstrate successful guidance in several non-line-of-sight scenarios where the drone begins at a position that is occluded from the light source.

II. Related Work

Drone Localization. Besides using traditional GPS / GPS-RTK based methods, researchers have explored RF methods to localize drones. However, most of these localization methods suffer from accuracy issues, with 3-D localization errors at best in 10s of centimeters. Additionally, GPS-based systems see limited accuracy in indoor scenarios and other types of wireless localization schemes (e.g., WiFi, ultra-wideband (UWB), active acoustic sensing) [11], [12], [13], [14] have limited operation range and require additional hardware support that palm-sized drones often cannot support computationally. Works that leverage vision to localize a drone often have limited field of view and see performance degradation in low-light conditions [15], [16]. Additionally, leveraging passive audio sensing to localize drones often suffers from the interfering noise of the propellers[17], [18].

Localization for Drone Landing. However, when the application requirements shift from general localization (needing to know (x, y, z)), into moving the drone onto a specific location, precise localization for drones becomes easier. To guide the drone to a landing target, researchers have leveraged markers, beacons, and anchors with varying modalities including UWB[19], [20] and visual objects and markers[21]. Placing a visual marker at the landing station reduces the landing problem to needing to estimate the relative location of the drone to the landing target[22]; as such, the most commonly used method for autonomously landing drones is to use RGB cameras on the drone to locate a pattern, usually a QR code, placed on the target landing location [23], [24]. These systems achieve high accuracy and have been deployed in commercial systems, such as in Google's project wing [25] for package deliveries. However, despite the high accuracy, camera-based approaches running computer vision algorithms incur a computational cost often not supported by small microdrones, and methods that leverage visible light often experience degraded performance in low-light conditions (e.g., at night) and cluttered scenarios (e.g., in an office or home setting). [26], [27] propose approaches that emit acoustic pulses to localize and guide drones. While this class of methods can overcome reduced performance observed by vision-based approaches in low-light scenarios, emitting a signal for active sensing requires additional payload and resources beyond what a typical microdrone can provide.

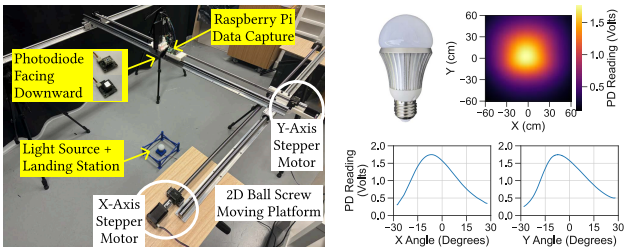

Fig. 2: Measuring light fields generated by IR light bulb.

Infrared Methods. There are several works that introduce IR-based methods for localization . Works that leverage IR to guide and land drones typically leverage IR tags[28], [29], [30] or LED matrices[31], [32], [33], [34] to create patterns that the drone can detect. These methods still require the use of a full IR camera, often in conjunction with other sensors such as RGB cameras, lidar, and IMU to be effective. This incurs heavy sampling, compute, and price cost. On the contrary, our work focuses on drone landing and guidance with only IR light. Additionally, we reduce the number of sensor channels from hundreds of thousands pixels to three or less, while providing accurate guidance without complex pattern recognition.

III. Method

Our approach is inspired by how moths, despite poor eyesight, navigate toward light by sensing changes in intensity. We focus on resource-constrained drones with a simple "one-pixel camera"—a photodiode.

A. Pilot Study with Simulation

We began with a simulation to validate the feasibility, using data from an actual infrared light source measured in the real world.

Experiment Setup: The measurement setup is illustrated in Figure 2 (left). It consists of a light source positioned at the center of a frame, which is constructed from two camera sliders arranged in a 2D grid. For data acquisition, a downward-facing photodiode (PD) was connected to a Raspberry Pi to collect light intensity readings. An HTC Vive VR controller[35] was used to obtain precise spatial locations for each measurement. The light field was measured at various heights by adjusting the vertical position of the light source relative to the ground.

Light Field Characterization: Figure 2 (right) shows the light field of a Commercial-Off-The-Shelf (COTS) IR light bulb at a specific height along with cross-sections on the

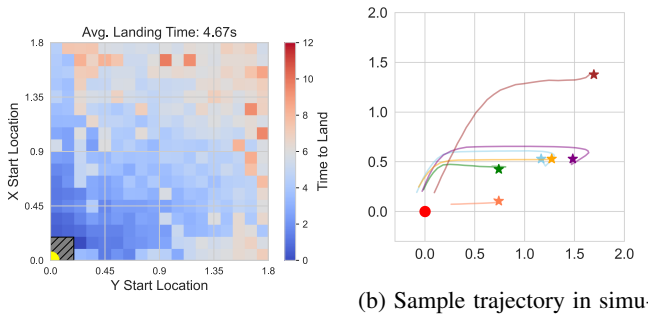

(a) Landing time.

(b) Sample trajectory in simulator with meter as unit.

Fig. 3: Landing performance simulated Gazebo.

X and Y axes. While we tested other light fields (using vertical-cavity surface-emitting laser (VCSEL) and diffuser lenses), the IR light bulb generates a field that is concave and centered around the light source, similar to a Gaussian curve. This concavity is ideal as it enables the drone to determine the direction of the landing target simply by moving toward increasing light intensity, without needing prior knowledge of the light field.

Gazebo Simulation: We built a drone landing simulator in Gazebo with a simple light-field gradient ascent algorithm. In the simulator, four photodiodes (PDs) are uniformly distributed around the drone, and their measurements are used to perform gradient ascent on the light intensity by commanding the drone's movement. In the simulation, the drone consistently hovered at or near the peak intensity (the light source), regardless of its starting location. Figure 3a shows the time required for the drone to reach the light source from various starting points up to 1.8 m away, confirming that the landing time is positively correlated with the initial distance. Six sample trajectories from different start locations are shown in Figure 3b, all of which successfully converge on the light source, indicated by the red dot at the origin.

B. Sensing from Drone

Building on the feasibility demonstrated in the previous simulation, this section addresses the practical design of the drone's on-board sensing system. We systematically investigate the optimal number and arrangement of photodiodes (PDs) required for landing.

Photodiode Sensing Configurations. There are intuitively two potential configurations: *Array of PDs (ArPD)* and *Single PD*, as shown in Figure 4.

a) Array of PDs (ArPD): Placing an array of PDs on the drone, that are spread out, allows the drone to leverage the spatial diversity to localize the direction of the light source. Figure 4a) shows an array of 6 PDs (ArPD 6). As an example, if the light source is on the left side of the drone, the PDs on the left side (PD3, 4 and 5) will see greater intensity, which will be the direction that the drone moves.

To determine the direction of drone movement, we represent the position of each photodiode (PD) as a unit vector $\hat{u}_i$ relative to a chosen reference point (e.g., the drone's center). Each vector is then scaled by the corresponding light intensity measurement PD_i, which reflects the measured light intensity at that PD. Summing these scaled vectors yields a resultant vector that captures the net directional influence of the light field. Finally, normalizing this vector ensures that the output $\vec{D}$ is a unit vector pointing in the overall direction of motion, as shown in equation $\vec{D} = \frac{\sum_{i=1}^{N} PD_i\,\hat{u}_i}{\left\|\sum_{i=1}^{N} PD_i\,\hat{u}_i\right\|}$.

b) Single PD: This configuration compensates for the lack of an array by utilizing the drone's mobility. By placing a single off-centered PD and sweeping 360 degrees along its yaw axis, as shown in Figure 4b, the drone effectively creates a virtual array by sampling the light field from multiple angles. The drone then identifies the direction of maximum intensity and moves towards it.

This approach presents a clear trade-off: while it reduces cost, power consumption and payload, these benefits sacrifice the time required for the drone to stop and perform a full rotation before each movement. More critically, the method's reliance on precise, controlled movements is a significant challenge for small drones. Their intricate control systems constantly make micro-corrections for motor variations, airflow disturbances, and sensor drift, leading to slight oscillations. These control inaccuracies, while minor, are difficult to correct and can severely degrade landing accuracy, particularly when the drone is close to the landing station and about to land.

Number of Photodiodes. We analyze the impact of the number of PDs on the landing performance using our drone and light field simulator (Section III-A). Figure 5 shows a heat map of the required time to land from different starting points in the x-y plane at a height of 1.1 m, as well as several example trajectories, while varying the number of PDs in the array. In all cases the drone is able to trace to the light source at origin regardless of the number of PDs being used. While the average landing time slightly increased as the number of PDs was reduced. The difference between using 3 PDs versus 6 is about 80 ms, which is almost negligible.

Angle of Photodiodes and Operating Range. In the previous measurements and simulations, we assumed that the PDs are facing downwards. However, PD readings depend significantly on the angle of the incident light on the sensor. This depends on 1) the distance away from the light source and 2) the angle of the PD on the drone, as illustrated in Figure 6. We take measurements at multiple distances from the light source, at a height of 1 m, and sweep the angle of the PD from 0 degrees (side facing) to 90 degrees (downward facing). When the drone is far from the light source (> 1.5 m), the PD sees the most light intensity when it is side-facing (0 degrees), since the incident angle of light on the sensor is smallest (e.g., the light is hitting the PD directly). However, as we move closer to the drone, we see that this peak shifts to a greater angle until the drone is within around 1 m. Within this range, the PD is completely downward facing (90 degrees) and measures the greatest light intensity. As we will see in Section V, the angle of the PD greatly impacts the operating distance or range from the landing station where Moth can reliably guide the drone.

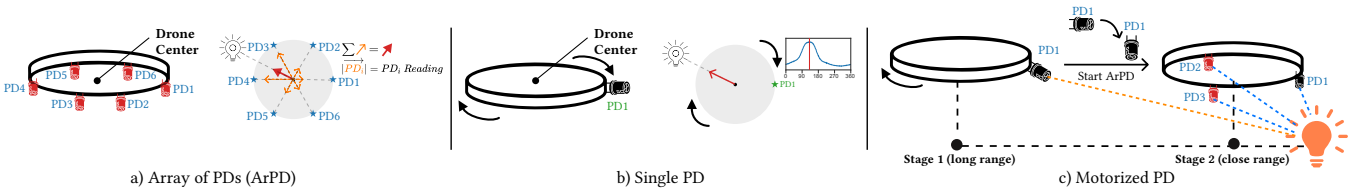

a) Array of PDs (ArPD) b) Single PD c) Motorized PD

Fig. 4: PD arrays, methods, and placements considered. a) array of PDs (6 shown) - ArPD6 and b) single PD where the drone sweeps 360 degrees along its yaw. c) Proposed motorized PD. When far from the landing station (> 1 m) Moth uses the motorized PD to guide the drone towards the landing station, while actuating the PD to the polar angle with the greatest intensity. When the drone is close to the landing station, the downward facing PDs measure greater light intensity and the Moth switches to using all three PDs as an array (ArPD) for the "final leg".

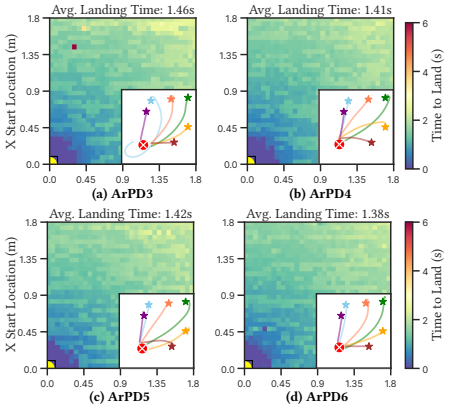

Fig. 5: Number of PDs vs landing time.

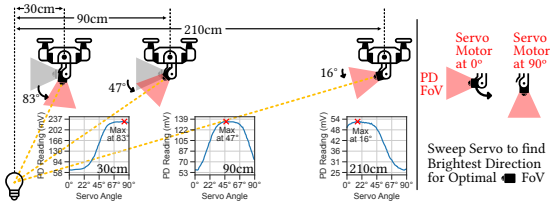

Fig. 6: Incident angle of light depends both on the angle of the PD on the drone and the distance from the landing station. High incident angle results in low intensity readings.

C. Proposed Motorized PD Approach

As discussed in the previous section, the angle of the PD should ideally be adjusted depending on how far away the drone is from the light source at the landing station. As such, we incorporate a motorized PD (MPD) whose angle can be tuned by the drone. Additionally, we also attach two additional downward PDs on the drone as shown in Figure 4c) in an equilateral triangle shape. We noticed that when the measured intensity of the two downward facing PDs exceeds the intensity of the motorized PD, the drone is within a distance from the landing station where an array of downward facing PDs can accurately guide the drone to land. This is because when the incident angle of light on the downward facing PDs is greater than an angled PD when the drone is close to the station as shown in Figure 6. Hence, we use these two additional PDs to determine when to switch from the single motorized PD to an array of PDs for the final leg. We use an array of PDs for the final leg, rather than a single PD. This method combines both the benefits of a single side facing PD, for guidance at long range, along with an array of downward facing PDs at short range.

The full landing procedure is as follows. The drone first performs a **yaw sweep**, spinning 360° in place and orienting the motorized PD toward the direction of maximum light intensity. It then conducts a **polar sweep**, adjusting the motorized PD across elevation angles and pointing it toward the angle of maximum intensity. During the **forward tracking** phase, the drone moves forward while dynamically adjusting the PD angle in proportion to the rate of increase in measured light intensity, ensuring continuous alignment with the source. Once the two downward-facing PDs measure a stronger intensity than the motorized PD, the system enters the **final leg**, where all three PDs function as an array of downward-facing PDs (ArPD) to guide the descent. Finally, when the intensities across all PDs converge, the drone is positioned directly above the light source and performs a controlled **descent** to complete the landing.

IV. Implementation

A. Platform for Sensing Light Fields on Drones

Hardware Platform. We implemented our design as a lightweight, attachable module, making it easily integrable with existing drones. As shown in Figure 7(a-b), we mounted it to a DJI Mini 2, where one motorized PD is installed at the front and the 6-PD array faces downward, arranged in a hexagonal pattern. We use the TI OPT101 PD throughout our design. To demonstrate our system's versatility and lightweight nature, we also created a palm-sized microdrone implementation with 3-PD array as shown in Figure 7(c).

Impact of IR Height Sensor. Drones commonly leverage IR sensors to measure the height from the ground. This typically involves emitting and measuring the response of IR pulses, which causes the measurements from the PDs to fluctuate as the laser turns on and off, as shown in Figure 8(a). To remove this interference, we take a rolling minimum average to capture PD measurements when the IR laser turns off and interpolate segments where the IR laser turns on.

B. Landing Station and Light Field Generation

Landing Station. To create the landing platform, we center the IR light bulb underneath a 20×25 cm sheet of clear anti-reflective glass that the drone will land on (as shown in Figure 7d). We measure the effect of the anti-reflective glass on the radiation pattern of the IR light bulb. Figure 7e shows the intensity of the light field as a function of distance from the center of the light source, at specific heights above the

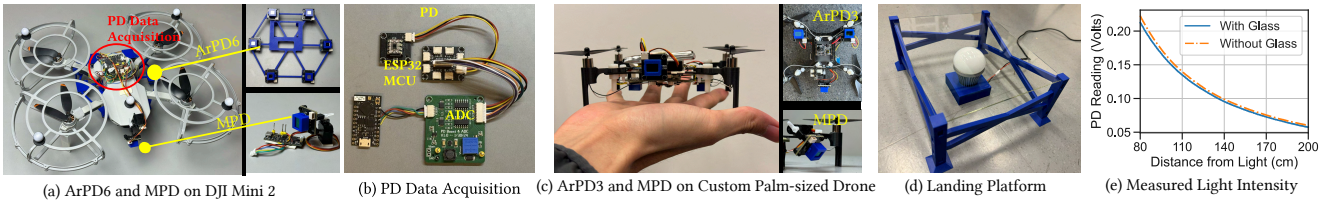

(a) ArPD6 and MPD on DJI Mini 2 (b) PD Data Acquisition (c) ArPD3 and MPD on Custom Palm-sized Drone (d) Landing Platform (e) Measured Light Intensity

Fig. 7: (a, b, c) Moth Implementation; (d) landing platform with anti-reflective glass; (e) Measured light intensity vs. distance with and without installing the glass landing platform, showing minimal impact of the anti-reflective glass to the light.

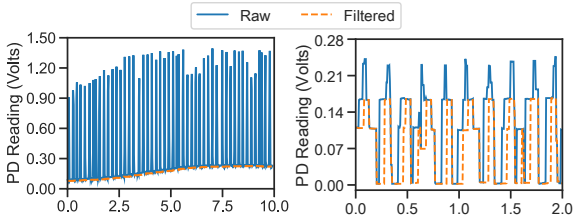

(a) Single Landing Station (No Modulation) (b) Multi Landing Station (w/ Modulation)

Fig. 8: The drone's IR height sensor emits IR pulses that cause large variations in PD measurements since it operates within the same range as our PD (860nm and 960nm). We apply a rolling minimum filter to remove this interference.

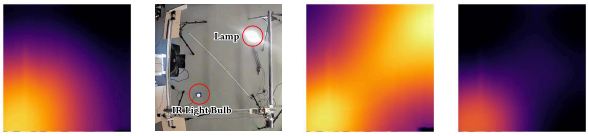

(a) No lamp (b) With lamp setup (c) With lamp (d) With lamp + filter

Fig. 9: Effect of external light sources.

light bulb, with and without the anti-reflective glass covering the light bulb. We see from our measurements that the glass has minimal effect on the radiation pattern.

External Light Sources. We also measure the effect of external light sources on the measured IR light field. Figure 9 shows our setup. We set a high powered lamp next to the IR light bulb and measure the light field at 1.1 m above the ground (Figure 9b). External light sources, like a lamp, can emit high amounts of IR light in addition to visible light. Using a spectrometer, we measured that the IR light bulb emits high energy near 940 nm. We place filters on top of our PDs to filter out light frequencies in other bands. The impact of the lamp has almost been completely removed after adding a 940 nm band pass filter (BPF) and an extra 780 nm low pass filter (LPF) (Figure 9d).

Outdoors. The sun is a major ambient source of IR light in outdoors scenarios. We observed that this causes the PD to saturate. However, applying our 940 nm BPF and 780 nm LPF, shown in Figure 10, reduces the noise floor significantly, and we can now observe changes in light readings caused by the IR light bulb. Figure 10 measures the X/Y cross section of our IR light field at various heights and indoors vs. outdoors. In gray, we high light the *operating range*, or the region above the noise level that is not flat. In this region PDs can sense light from the landing station and guide the drone. We see that this range varies depending on the height of the drone from the ground, as well as the orientation of the PDs, as we will discuss in Section V.

We see that the measured light field outdoors is almost identical to the indoor scenario, except with a DC offset caused by the extra environment light. Because our method relies on light gradients or changes, rather than absolute intensities to determine the drone's moving direction, DC offset slightly affects the performance of our system. Moreover, the potential *operating range* of Moth also remains unaffected between different lighting conditions. In summary, **Moth remains largely immune to different lighting conditions or external sources of light in the environment**.

C. Multiple Landing Stations

Certain applications may require drones to land at different landing stations, which our current approach using standard infrared light bulbs cannot satisfy. To distinguish between landing targets, we apply a frequency-division multiplexing approach: each landing station emits light at a distinct frequency through a modulation module (Figure 11 (a)), while the drone applies a rolling minimum filter on the PDs to remove interference from the height sensor (Figure 8 (b)).

In our experiments, we set two landing stations to emit at 5 Hz and 7 Hz, then applied a 512-point Fast Fourier Transform (FFT) to separate the signals from each landing station. Figure 11 (b) shows the FFT output when the drone hovers above 5 Hz station with the signal from 7 Hz station mixed in. The peak at these frequencies remained consistent both with and without the drone's IR light sensor noise, showing minimum influence to FFT of the rolling minimum filter described in Section IV-A.

To verify that modulation maintains system accuracy, we measured angle estimation error of the ArPD and MPD algorithm, as shown in Figure 11 (c-d). Although FFT introduces some noise, the accuracy is largely unaffected. The FFT demodulation is implemented on the PD data acquisition ESP32-S3 microcontroller, achieves a computation latency of 2.079 ms, enabling real-time operation.

V. Experiments

Final Leg Benchmarking. Figure 12 shows the estimated direction of greatest light intensity using an array of 3 and 6 downward facing PDs (ArPD3 and ArPD6) at various locations around the landing station, during the final leg, with the drone hovering at 1 m. Due to symmetry and limited space, we only present data from the first quadrant. We take the ArPD6 and ArPD3 measurements in a real indoor deployment on a DJI Mini 2 (ArPD6, Figure 7(a)) and custom designed palm-sized drone (ArPD3, Figure 7(c)),

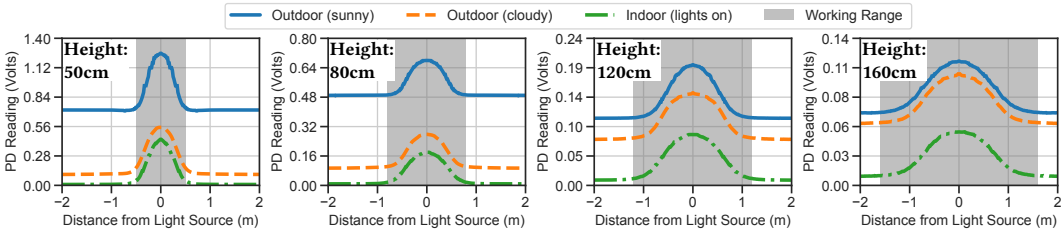

Fig. 10: Effect of external sunlight on noise floor of measured light from PD.

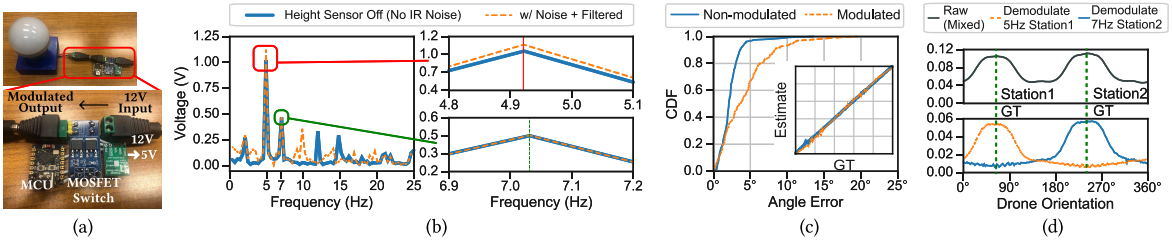

(a) (b) (c) (d)

Fig. 11: (a) Landing station modulation module; (b) FFT comparison of received light signals with and without interference from drone's IR height sensor, measured during hover over 5Hz-modulated landing station with 7Hz station in proximity; (c) ArPD angle error comparison between modulated and unmodulated landing stations; (d) MPD signals after 360° rotation: raw signal showing two indistinguishable peaks from both stations, compared with signals after 5Hz and 7Hz demodulation.

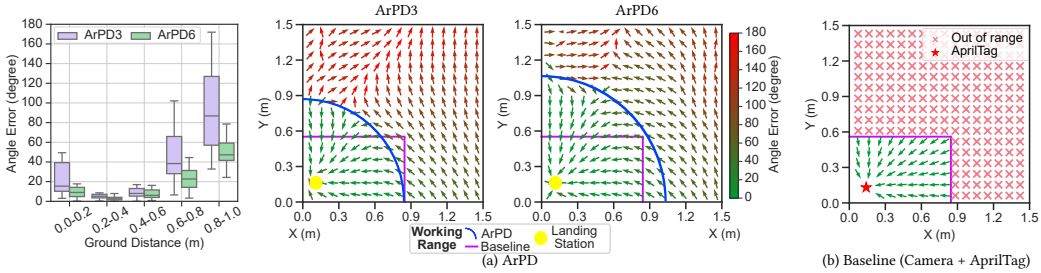

Fig. 12: Estimated movement directions at 1 m height for a) ArPD and b) camera baseline.

described in Sections IV and V. A vision landing baseline is implemented on the DJI Mini2 drone using its RGB camera and AprilTag. The baseline method has a rectangular operating range due to the rectangular nature of images. For our proposed approach, we see that adding more PDs increases the working range of the downward facing PDs (from 0.9 to 1.1 m). However, leveraging 3 PDs still gives a greater range than the baseline.

Operating Range. Further differences between IR and RGB-based approaches arise when looking at the operating range in which each method can achieve these low errors; outside of these ranges, the drone can no longer reliably detect the location of the landing station. Figure 13 shows the raw light intensity measurement sweeping 360 degrees along the drone's yaw axis, while hovering at 1.2 m. We see that the upper and lower bounds of the operating range of the downward facing (used in ArPD) and motorized PD, respectively, are at 0.9 m away from the landing station, which is exactly complementary to one another. We observed that *the motorized PD can still detect the direction of the light source up to around* 40 *m*, where it reaches the limit of the resolution of the analog-to-digital converter (ADC) and far exceeds the range of our vision baseline.

End-to-End. Figure 14 shows the end-to-end landing time, landing location distance error, and distribution of landing locations when deploying Moth in a real indoor setting with normal room light. We compare palm-sized microdrone-based ArPD3, COTS DJI Mini2-based ArPD6 against an RGB-camera-based solution.

The CDF of direction estimation errors measures errors within the "operating range" where each method is capable of accurately detecting and guiding the drone to the light source. The landing time plots also reflect just this region.

At a typical height of around 1 m, Moth can reliably guide the drone within 11.1 m to the landing station, as it leverages complementary mechanisms (MPD when far and ArPD when close) to cover the range, while camera-based method fails past 1.07 m.

Landing accuracy and time. The average landing time and error for each method within their respective operating ranges are: *ArPD3 (7.1 s, 9.2 cm)* , *ArPD6 (7.3 s, 7.3 cm)*, and the *baseline AprilTag method (8.3 s, 9.4 cm)*. Metrics for the motorized PD are not reported because it is used to guide the drone to the "final leg", within 1.1 m, before switching to ArPD, which is much more accurate at close distances. ArPD3 achieves slightly lower landing error

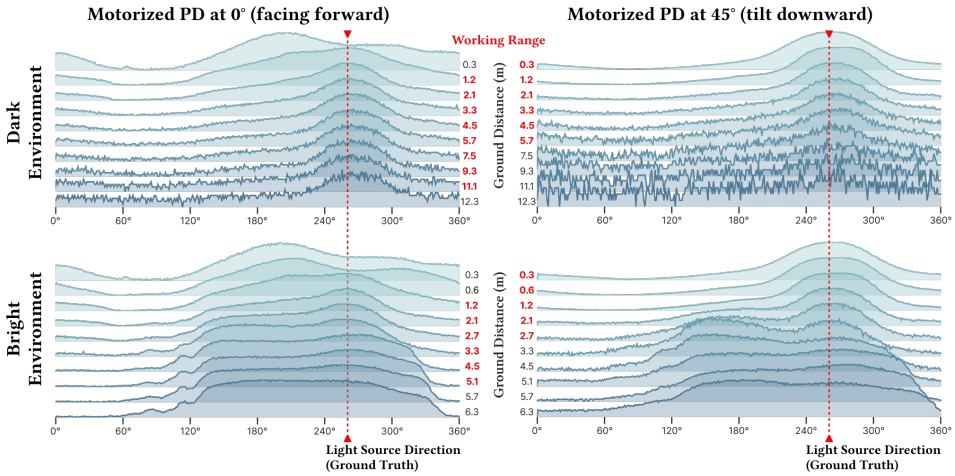

Fig. 13: Light intensity measurements at different distances from the landing station sweeping 360 degrees around the drone's yaw axis. a) a side facing PD (0 degrees) and b) a downward facing PD (90 degrees). The ranges in which these two PDs can accurately measure the direction of the light source are exactly orthogonal.

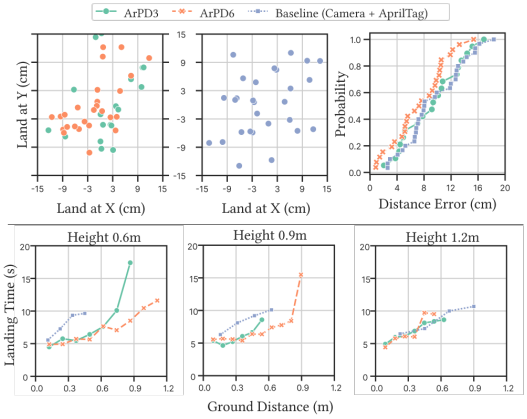

Fig. 14: End-to-end landing time and accuracy comparison. Top shows scatterplot and CDF for landing locations and error. Bottom shows landing time against ground distance of landing start point at different heights.

than the baseline camera-based method at a faster speed. Increasing the number of PDs, ArPD6 has slightly higher accuracy with similar landing time.

Power Consumption. The entire Moth system consumes less than 0.5 W. This total is composed of the main ADC+WiFi+MCU module (423.29 mW), the Fast Fourier Transform (FFT) computation (23 mW), the servo motor (idle 30 mW and 301 mW during actuation) and the three photodiodes (PDs), which each add between 330 µW and 720 µW depending on the received light strength. This power draw is negligible on drones, whose motors consume Watt-level power (roughly 50 W for the DJI Mini 2 and 30 W for Moth's custom drone). Consequently, after outfitting the DJI Mini 2 with Moth, there was no noticeable change to the drone's battery life.

VI. Discussion

Optimizing Methods and Algorithms. The landing methods proposed in this work guide the drone directly above the landing station, before descending, essentially estimating 2D

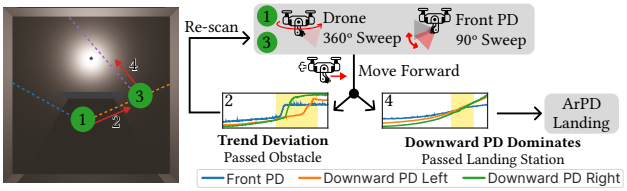

Fig. 15: NLOS navigation example process.

light gradients. In future work, we plan to explore more array layouts and methods that allow the drone to travel in three dimensions, enabling the system to descend while traveling to the landing station. This could potentially reduce landing errors and landing time by removing the final descent once the drone lands at the center of the landing pad.

Extending to NLOS Navigation. The proposed method in Moth also shows promise for navigating in partially non-line-of-sight (NLOS) conditions, such as moving through a doorway into an adjacent room. In these scenarios, the drone navigates by treating openings as intermediate pseudo-light sources, using the same method in the landing cases as illustrated in Figure 15. Upon reaching the opening and entering the direct LOS of the landing station, the drone's photodiodes detect an exponential jump in light intensity. This distinct signal is used as a cue for the drone to stop, reorient itself toward the actual landing station, and begin its final approach.

VII. Conclusion

We propose Moth, a light-weight, efficient, and bio-inspired method for landing and guiding drones using IR light. Unlike existing vision-based and IR-based approaches, Moth requires only an off-the-shelf IR light bulb, with no modifications, at the landing station, and a small array of three PDs on the drone, costing under 83 USD. To leverage only a few PDs, we exploit the mobility of the drone to move the PDs spatially, creating a virtual array and guiding the drone towards the light source. Through our experiments, we show that Moth can accurately land drones up to 11.1 m

away, which is $9.3\times$ greater in range than traditional marker-based methods from the same height. We also demonstrate that Moth can help guide and navigate drones in partial non line of sight scenarios. Moth is a critical step towards low cost and low energy drone guidance for indoor environments.

ACKNOWLEDGMENT

This research was partially supported by COGNISENSE, one of seven centers in JUMP 2.0, a Semiconductor Research Corporation (SRC) program sponsored by DARPA, as well as the National Science Foundation under Grant Number CNS-1943396. The views and conclusions contained here are those of the authors and should not be interpreted as necessarily representing the official policies or endorsements, either expressed or implied, of Columbia University, NSF, SRC, DARPA, or the U.S. Government or any of its agencies.

REFERENCES

[1] S. De Silvestri, M. Pagliarani, F. Tomasello, D. Trojaniello, and A. Sanna, "Design of a service for hospital internal transport of urgent pharmaceuticals via drones," *Drones*, vol. 6, no. 3, p. 70, 2022.

[2] Y. Pan, J. Gao, J. Duan, J. Shi, B. Guo, Y. Liang, and Y. Hu, "Pioneering cooperative air-ground instant delivery using uavs and crowdsourced couriers," *Proceedings of the ACM on Interactive, Mobile, Wearable and Ubiquitous Technologies*, vol. 8, no. 4, 2024.

[3] H. Kolamunna, T. Dahanayaka, J. Li, S. Seneviratne, K. Thilakaratne, A. Y. Zomaya, and A. Seneviratne, "Droneprint: Acoustic signatures for open-set drone detection and identification with online data," *Proceedings of the ACM on Interactive, Mobile, Wearable and Ubiquitous Technologies*, vol. 5, no. 1, pp. 1–31, 2021.

[4] M. Javaid, I. H. Khan, R. P. Singh, S. Rab, and R. Suman, "Exploring contributions of drones towards industry 4.0," *Industrial Robot: the international journal of robotics research and application*, vol. 49, no. 3, pp. 476–490, 2022.

[5] H. Jahani, Y. Khosravi, B. Kargar, K.-L. Ong, and S. Arisian, "Exploring the role of drones and uavs in logistics and supply chain management: a novel text-based literature review," *International Journal of Production Research*, pp. 1–25, 2024.

[6] H. Abdelnasser, M. Heggo, O. Pang, M. Kovac, and J. A. McCann, "Radro: Indoor drone tracking using millimeter wave radar," *Proceedings of the ACM on Interactive, Mobile, Wearable and Ubiquitous Technologies*, vol. 8, no. 3, pp. 1–23, 2024.

[7] M. Zhao, J. Xia, K. Hou, Y. Liu, S. Xia, and X. Jiang, "Rasp: A drone-based reconfigurable actuation and sensing platform towards ambient intelligent systems," *arXiv preprint arXiv:2403.12853*, 2024.

[8] G. Chen, X. Yu, N. Ling, and L. Zhong, "Typefly: Flying drones with large language model," *arXiv preprint arXiv:2312.14950*, 2023.

[9] S. Z. E. C. LTD, "Open source quadcopter minifly drone flight control stm32 diy kit," https://www.aliexpress.us/item/1005005961290267.html, Feb 2024, accessed: 2024-03-11.

[10] W. Giernacki, M. Skwierczyński, W. Witwicki, P. Wroński, and P. Kozierski, "Crazyflie 2.0 quadrotor as a platform for research and education in robotics and control engineering," in *2017 22nd International Conference on Methods and Models in Automation and Robotics (MMAR)*. IEEE, 2017, pp. 37–42.

[11] A. Dhekne, A. Chakraborty, K. Sundaresan, and S. Rangarajan, "TrackIO: Tracking first responders Inside-Out," in *16th USENIX Symposium on Networked Systems Design and Implementation (NSDI 19)*. Boston, MA: USENIX Association, Feb. 2019, pp. 751–764.

[12] G. Chi, Z. Yang, J. Xu, C. Wu, J. Zhang, J. Liang, and Y. Liu, "Wi-drone: wi-fi-based 6-dof tracking for indoor drone flight control," in *Proceedings of the 20th Annual International Conference on Mobile Systems, Applications and Services*, 2022, pp. 56–68.

[13] Y. Sun, W. Wang, L. Mottola, R. Wang, and Y. He, "Aim: Acoustic inertial measurement for indoor drone localization and tracking," in *Proceedings of the 20th ACM Conference on Embedded Networked Sensor Systems*, 2022, pp. 476–488.

[14] A. Famili, A. Stavrou, H. Wang, and J.-M. Park, "idrop: Robust localization for indoor navigation of drones with optimized beacon placement," *IEEE internet of things journal*, 2023.

[15] M. Pavliv, F. Schiano, C. Reardon, D. Floreano, and G. Loianno, "Tracking and relative localization of drone swarms with a vision-based headset," *IEEE Robotics and Automation Letters*, vol. 6, no. 2, pp. 1455–1462, 2021.

[16] E. Mráz, J. Rodina, and A. Babinec, "Using fiducial markers to improve localization of a drone," in *2020 23rd International Symposium on Measurement and Control in Robotics (ISMCR)*. IEEE, 2020.

[17] W. Manamperi, T. D. Abhayapala, J. Zhang, and P. N. Samarasinghe, "Drone audition: Sound source localization using on-board microphones," *IEEE/ACM Transactions on Audio, Speech, and Language Processing*, vol. 30, pp. 508–519, 2022.

[18] G. Chen, N. Weiner, and L. Zhong, "Pod: A smartphone that flies," in *Proceedings of the 7th Workshop on Micro Aerial Vehicle Networks, Systems, and Applications*, 2021, pp. 7–12.

[19] A. Ochoa-de Eribe-Landaberea, L. Zamora-Cadenas, O. Peñagaricano-Muñoa, and I. Velez, "Uwb and imu-based uav's assistance system for autonomous landing on a platform," *Sensors*, vol. 22, 2022.

[20] Q. Zeng, Y. Jin, H. Yu, and X. You, "A uav localization system based on double uwb tags and imu for landing platform," *IEEE Sensors Journal*, 2023.

[21] C. Kim, E. M. Lee, J. Choi, J. Jeon, S. Kim, and H. Myung, "Roland: Robust landing of uav on moving platform using object detection and uwb based extended kalman filter," in *2021 21st International Conference on Control, Automation and Systems (ICCAS)*. IEEE, 2021, pp. 249–254.

[22] C. G. Grlj, N. Krznar, and M. Pranjić, "A decade of uav docking stations: A brief overview of mobile and fixed landing platforms," *Drones*, vol. 6, no. 1, p. 17, 2022.

[23] J. Wang, D. McKiver, S. Pandit, A. F. Abdelzaher, J. Washington, and W. Chen, "Precision uav landing control based on visual detection," in *2020 IEEE Conference on Multimedia Information Processing and Retrieval (MIPR)*. IEEE, 2020, pp. 205–208.

[24] P. H. Nguyen, M. Arsalan, J. H. Koo, R. A. Naqvi, N. Q. Truong, and K. R. Park, "Lightdenseyolo: A fast and accurate marker tracker for autonomous uav landing by visible light camera sensor on drone," *Sensors*, vol. 18, no. 6, p. 1703, 2018.

[25] P. Wing, "Project wing," https://wing.com/, Sept 2023, accessed: 2023-09-29.

[26] W. Wang, L. Mottola, Y. He, J. Li, Y. Sun, S. Li, H. Jing, and Y. Wang, "Micnest: Long-range instant acoustic localization of drones in precise landing," in *Proceedings of the 20th ACM Conference on Embedded Networked Sensor Systems*, 2022, pp. 504–517.

[27] Y. He, W. Wang, L. Mottola, S. Li, Y. Sun, J. Li, H. Jing, T. Wang, and Y. Wang, "Acoustic localization system for precise drone landing," *IEEE Transactions on Mobile Computing*, 2023.

[28] J. Springer, G. Þ. Guðmundsson, and M. Kyas, "A precision drone landing system using visual and ir fiducial markers and a multi-payload camera," *arXiv preprint arXiv:2403.03806*, 2024.

[29] I. Kalinov, E. Safronov, R. Agishev, M. Kurenkov, and D. Tsetserukou, "High-precision uav localization system for landing on a mobile collaborative robot based on an ir marker pattern recognition," in *2019 IEEE 89th Vehicular Technology Conference (VTC2019-Spring)*. IEEE, 2019, pp. 1–6.

[30] V. Khithov, A. Petrov, I. Tishchenko, and K. Yakovlev, "Toward autonomous uav landing based on infrared beacons and particle filtering," in *Robot Intelligence Technology and Applications 4: Results from the 4th International Conference on Robot Intelligence Technology and Applications*. Springer, 2017, pp. 529–537.

[31] W. Kong, D. Zhang, X. Wang, Z. Xian, and J. Zhang, "Autonomous landing of an uav with a ground-based actuated infrared stereo vision system," in *2013 IEEE/RSJ international conference on intelligent robots and systems*. IEEE, 2013, pp. 2963–2970.

[32] T. Yang, G. Li, J. Li, Y. Zhang, X. Zhang, Z. Zhang, and Z. Li, "A ground-based near infrared camera array system for uav auto-landing in gps-denied environment," *Sensors*, vol. 16, no. 9, p. 1393, 2016.

[33] J. Janousek and P. Marcon, "Precision landing options in unmanned aerial vehicles," in *2018 International Interdisciplinary PhD Workshop (IIPhDW)*. IEEE, 2018, pp. 58–60.

[34] E. Nowak, K. Gupta, and H. Najjaran, "Development of a plug-and-play infrared landing system for multirotor unmanned aerial vehicles," in *2017 14th Conference on Computer and Robot Vision (CRV)*. IEEE, 2017, pp. 256–260.

[35] H. Corporation, "Htc vive - vr, ar, and mr headset, glasses, experiences," https://www.vive.com/us/, Jun 2009, accessed: 2024-03-14.